Paper III

Severe winds in the Nordic Seas: a QuikSCAT climatology with emphasis on the marginal ice zone off the east coast of Greenland

Erik W. Kolstad
Bjerknes Centre for Climate Research
Allégaten 70
5007 Bergen
Norway

Manuscript
31 January, 2007

Abstract

In this paper high-resolution satellite-derived QuikSCAT wind data is used to provide a climatology of both average and extreme winds in the Nordic Seas. In addition to a number of known features, such as the persistent, strong northerlies over the Greenland Sea, the remarkably strong barrier winds in the Denmark Strait and the surface jet near the southern tip of Spitsbergen, several new features were identified. Most importantly, it was shown that:

1) the winds in the marginal ice zone on the east coast of Greenland are consistently amplified in a narrow band near the ice edge, with exceptionally high extreme values;

2) these winds coincide with regions with a high frequency of reverse-shear conditions, i.e. the actual winds are in the opposite direction of the thermal wind. Such conditions are known to be favourable for strong surface heat and momentum fluxes;

3) there is a wind speed maximum in the region where the Odden sea-ice feature usually forms along the east coast of Greenland;

4) there is a wind shadow, largely undetected by the NCEP reanalysis and most likely caused by the topography of Greenland, to the northeast of Iceland along the Northeast Atlantic storm track. A similar feature is found in the Barents Sea.

1 Introduction

In this paper, a 7-8-yr wind climatology of the Nordic Seas is compiled using high-resolution satellite-derived QuikSCAT wind data, which are available on a sufficiently high horizontal resolution to represent small-scale systems. The Nordic Seas is a region where mesoscale weather phenomena may have a large impact on both the average and the extreme surface winds, of which there exists no systematic study to date. Because of the projected increased human activity, knowledge about the nature of the regional winds is crucial in itself. In addition, due to the possible feedback mechanisms between winds and sea-ice movement, surface heat fluxes and thus the atmospheric circulation, the near-surface oceanic mixing and surface ocean currents,it is also important for the understanding of couplings to larger scales.

The sea surface in the Nordic Seas (the Northeast Atlantic Ocean north of Iceland) is uniquely warm compared to other oceanic regions at similar latitudes (Figure 1). This is because the North Atlantic Current (Blindheim and Østerhus, 2005) brings warm water masses from the south, but also because of persistent large-scale atmospheric circulation patterns (Furevik and Nilsen, 2005; Sorteberg et al., 2005). The most dominant of these is the North Atlantic Oscillation (NAO; Rogers, 1997; Hurrell et al., 2006).

The wind field in the Nordic Seas is strongly influenced by the Atlantic westerly storm track. Hoskins and Hodges (2002) tracked cyclones over a 22-yr period and found that, on the synoptic scale, the primary genesis regions are found just east of the Rocky mountains and to the east of the North American continent. A strong secondary genesis region was identified over the Nordic Seas, with very high growth rates. During winter, distinct maxima of cyclone counts are found over the Norwegian and Barents Seas (Zhang et al., 2004; Wernli and Schwierz, 2006). The large air-sea temperature differences near the sea-ice edge or during marine cold-air outbreaks give rise to mesoscale phenomena such as polar lows (Rasmussen and Turner, 2003), but are also favourable for cyclone intensification on a larger scale.

There exist few climatological studies of small-scale cyclones in the Nordic Seas. Harold et al. (1999a,b) inspected satellite images over a 2-yr period manu-

ally, and found that wintertime cyclones with a diameter of 200-400 km occurred most frequently in the Norwegian Sea and to the south of the Denmark Strait. The slightly larger cyclones (400-600 km) were primarily found over the Greenland Sea. In a study of cyclones that were detectable in the ERA-40 data set in the same period, Condron et al. (2006) found centres of action west of Spitsbergen (at the southern entrance to the Fram Strait), over the northern Norwegian Sea, over the Greenland Sea near Jan Mayen, and just south of Iceland. The strongest cyclones were found over the Greenland Sea and west of Spitsbergen.

A number of individual regional phenomena have also been addressed in the literature. Two wind maxima at either end of the Denmark Strait were identified by Moore and Renfrew (2005), and were found to be cause by orographic forcing from Greenland and Iceland. Similar topographic jets have been found in easterly flow over both the southern (Skeie and Grønås, 2000) and northern (Sandvik and Furevik, 2002) tips of Spitsbergen and along the west coast of Norway in southwesterly flow Barstad and Grønås (2005). Near the east coast of Greenland, katabatic winds have been identified and analysed by Klein and Heinemann (2002).

Polar lows in the Nordic Seas have also been studied extensively. In what is probably the first written account of these maritime cyclones, the priest Petter Dass described what could only have been polar lows in the late 1600s. Since satellite data became routinely available, the term 'polar low' or 'polar mesocyclone' has been used to define a range of features, which is often referred to as the 'polar low spectrum' (Rasmussen and Turner, 2003).

At least one of the members of the spectrum has received little attention in the literature. The leading edges of cold-air outbreaks are usually referred to as Arctic fronts (Shapiro and Fedor, 1989; Shapiro et al., 1989; Grønås and Skeie, 1999) (and sometimes as boundary-layer fronts; Drue and Heinemann, 2001, 2002). When strongly stable air from over the ice is advected over a warm sea surface, a shallow boundary layer develops as the air masses are eroded by surface heat fluxes from below. The wind speed over the ocean surface at the front depends on a number of factors and feedback mechanisms. If the surface wind speed is strong, the newly heated air is replaced by new, cold air and heat fluxes are enhanced, which is a positive feedback on the winds.

The surface winds in the marginal ice zone along the east coast of Greenland are known for their fierceness and directional persistence. In a northeasterly storm during the Easter of 1952, seven Norwegian sealing vessels went down. Five of these were never found, and a total of 79 sailors lost their lives. On 9 April 1933, a wind gust of 163 knots (84 ms^{-1}) was recorded on the island of Jan Mayen, one of the strongest winds ever measured by conventional means (Lamb, 1991).

Further east, in the Norwegian and Barents Seas, the human activity is more frequent. Rough weather due to extratropical cyclones, polar lows, Arctic fronts or other mesoscale phenomena, have proved fatal for many sailors (342 in the last century, according to Grønås and Skeie, 1999). A numerical simulation performed at the Geophysical Institute in Bergen, Norway, suggested that an Arctic front with hurricane-force winds was present nearby when the British trawler Gaul went down south of Bjørnøya (Bear Island) in 1974, killing 36 (Are Norhagen, M. Sc. thesis).

Økland (1998) presented an idealised model showing that mesoscale frontal processes can amount to another positive feedback on the surface winds. An actual case from 1993, where a coast guard ship in the vicinity of Bjørnøya was surprised by a sudden strengthening of the easterly wind field, was studied in detail. An east-west-oriented ice edge and an initial easterly wind along this edge were prescribed. By imposing an invariant sensible heat flux of 500 Wm^{-2} over the sea surface, the model yielded both a frontogenetic cross-frontal vertical circulation (land breeze) and an amplification of the easterly wind speed on the order of 10 ms^{-1}. This solution was in good agreement with the ship observations. Based on his findings, Økland (1998) suggested that the 1952 disaster in the Greenland Sea was caused by a rapid amplification of the northerly winds along a front near the ice edge.

Grønås and Skeie (1999) studied the same case in more detail using a high-resolution numerical limited-area model. They found that the temperature difference between the air and the sea surface in the region of the most intense cold-air advection was 30 K. With a surface wind speed of 25 ms^{-1}, this yielded sensible heat fluxes on the order of 1200 Wm^{-2}, more than double the value used by Økland (1998). (Pagowski and Moore (2001) claimed that heat fluxes in mesoscale models are sometimes exaggerated, and this number should be treated

with caution.) In spite of this, the simulated surface wind speed was lower than the one that was observed. The simulated 1000 hPa geostrophic wind speed was on the order of 70 ms^{-1}, but due to surface friction, the strongest simulated actual winds were found in a low-level jet with hurricane-force winds at the top of the boundary layer. Near the surface, the highest simulated wind speed was just under 30 ms^{-1}.

The low-level baroclinicity in the marginal ice zone is dictated by the spatial structure of the sea-ice, and the thermal wind is directed along the ice from south to north. In the case described above, the mean flow was in the opposite direction. To maintain thermal wind balance in such conditions, a vertical geostrophic wind shear, with the wind speed decreasing with height, is required. Such conditions were termed reversed shear flow by Duncan (1978) as "uniform, horizontal flow in which the mean wind at a given level is parallel but opposite in direction to the thermal wind at that level" (hence the designation 'reversed'). He also stated that in reversed shear flow, the surface fluxes of momentum, heat and moisture are enhanced compared to "the more normal flow".

The combination between reverse shear and large temperature gradients near the surface leads to strong surface winds and substantial heat fluxes from the sea to the atmosphere, depending on the sea surface temperatures, the air temperature and static stability over the ice, as well as the surface wind speed and direction. Kolstad (2006) found that wintertime low-level reverse-shear conditions in the Nordic Seas were most frequently found near the ice edge over the western part of the Barents Sea (> 30 % of the time from November to March), over the Greenland Sea (> 30 %) and in the Denmark Strait (40 %).

On the basis of the high frequency of reverse-shear conditions near the ice edge and the results from the mesoscale analysis by Økland (1998) and Grønås and Skeie (1999), we hypothesise that Arctic fronts or similar small-scale features form regularly in the marginal ice zone both off the east coast of Greenland in northerly flow and in the Barents Sea in easterly flow, leading to strong surface winds.

The potential existence of a wind regime in the marginal ice zone may hold implications for the understanding of: 1) large-scale sea-ice movement in the region. Wu et al. (2004) and Bengtsson et al. (2004) found a negative correlation

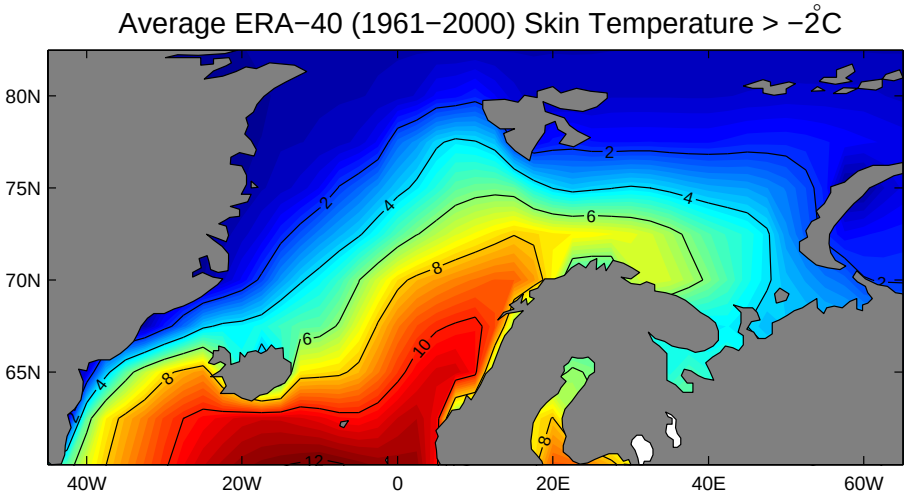

Figure 1: This is a combined representation of the sea surface temperatures and the sea-ice extent in the Nordic Seas. ERA-40 (Kållberg et al., 2004) skin temperature is defined as SST over open ocean and as the temperature of the surface (including sea-ice) elsewhere. In order to mask the large negative contribution from the surface temperature over sea-ice, we show the average exceedance over -2°C (the approximate freezing point) throughout the year. If there is ice 100 % of the time, the value is zero.

between sea-ice extent and sea level pressure in the Greenland-Barents Sea region and suggested that the resulting circulation (land breeze) exerted a positive feedback on the ice; 2) sea-ice features such as "Odden" between Greenland and Jan Mayen (Shuchman et al., 1998; Comiso et al., 2001), whose ice dynamics have been shown to be entirely wind-driven (Wilkinson, 2006), or the rapidly forming sea-ice tongue east of Spitsbergen (Nghiem et al., 2005); 3) the direct feedback on near-surface ocean currents in terms of wind stress forcing near the ice edge; 4) the magnitude of the surface fluxes in the marginal ice zone. The heat transfer from the ocean to the atmosphere is an important feedback mechanism on the surface winds (e.g. Bresch et al., 1997; Økland, 1998); 5) surface winds in sea-ice regions in other regions such as the Labrador Sea, the Bering Sea, and not least in Antarctica.

2 Data and method

The QuikSCAT satellite-derived surface wind observations are available on a twice-daily basis (morning and evening) over the entire globe, starting in July 1999. We used data through December 2006. Surface wind speed and wind direction are retrieved from satellite measurements of radar backscatter from the sea surface. In consequence, no data is available over sea-ice and land. A thorough introduction to the QuikSCAT data is given by Hoffman and Leidner (2005).

QuikSCAT data are produced by Remote Sensing Systems (REMSS) and sponsored by the NASA Ocean Vector Winds Science Team. Data are available at http://www.remss.com. The resolution is 0.25 by 0.25 degrees, which is equivalent to 28 km in the meridional direction and 7 km in the zonal direction at latitude 75N. Each grid cell covers an area of roughly 200 km^2. The validity of the QuikSCAT data for cases with high wind speeds and in the vicinity of the sea-ice edge is discussed in the next section.

The average wind field relative to the ice edge was computed as follows. For each QuikSCAT sample, the first valid values when searching towards the east from the coast of Greenland was located for each latitude. This corresponds to the first open-ocean grid cell in the Greenland Sea. When there is much sea-ice, such as in late winter, the left edge of the coordinate system relative to the ice edge is oriented from roughly southwest to northeast (along the edge).

The NCEP reanalysis data (NCEP-R from now on; Kalnay et al., 1996) were used for the synoptic analysis in this paper. This choice was made quite simply because these data are available during the whole QuikSCAT period, whereas the ECMWF ERA-40 Kållberg et al. (2004) period was terminated in 2002.

The timing of the QuikSCAT sampling varies on a daily basis. This makes it difficult to compare the QuikSCAT data directly to 6-hourly reanalysis products. However, manual inspection of the QuikSCAT recording time shows that the morning samples are usually taken between UTC 0400 and UTC 0800 in the Northeast Atlantic, while the evening samples are generally taken between 1900 UTC and midnight. When comparing QuikSCAT winds with reanalysis data, the morning (evening) passes were taken to be represented by the UTC 0600 (1800) samples.

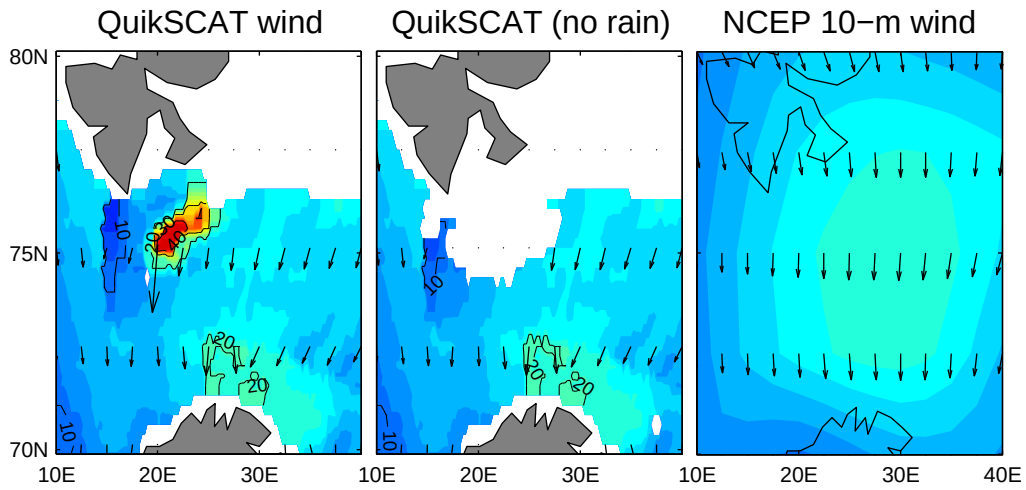

Figure 2: QuikSCAT surface wind and NCEP-R 10-metre wind on the morning (0600 UTC for NCEP-R) of 25 February 2005.

3 On the validity of QuikSCAT winds

Before presenting the wind climatology, it is appropriate to discuss the possible errors in the QuikSCAT wind data. It is known that the presence of rain may contaminate the QuikSCAT surface wind speed retrieval process (Chelton et al., 2006). The errors in both wind speed and wind direction decrease with high wind speeds (see also Hoffman and Leidner, 2005; Leslie and Buckley, 2006), but the validity of the wind field should ideally be assessed manually on a case by case basis. This is not feasible in this study, where large amounts of data are processed automatically. Manual inspection of cases with severe wind speed in the study area suggests that the errors due to rain alone are small enough to be negligible for the purposes of this paper.

However, there is also a concern that pixels in the marginal ice zone may be incorrectly interpreted by the QuikSCAT algorithms. On the REMSS web page, an example of too high wind speeds over undetected sea-ice in the Black, Caspian and Aral Seas is given. In the Nordic Seas, we have compared QuikSCAT wind maps with satellite images and sea-ice maps from the Norwegian Meteorological Office, and found that a 'safety margin' is kept near the ice edge by deleting the

first few pixels in the marginal ice zones. However, in some cases sea-ice clearly goes undetected. An example from the Norwegian and Barents Seas is given in Figure 2. The 'raw' QuikSCAT winds are shown to the left, while rain-flagged values have been removed in the middle panel. It is virtually certain that the unrealistically high wind speed values between Hopen and Bjørnøya are due to sea-ice 'interference'. The high values are situated over the shallow Svalbard Bank, where sea-ice is known to form rapidly when conditions are right (Nghiem et al., 2005). Although not shown here, maps of the neighboring samples also have high wind speeds, even though the overall wind situation was different. When rain-flagged pixels are removed, the high wind speeds disappear. Although it is perhaps overly prudent, in light of this example and others not shown, we chose to eliminate all rain-flagged pixels from the climatological analysis below.

4 Results

4.1 Average wind field in the Northeast Atlantic

In Figure 3, the average wintertime QuikSCAT wind speed for two months at a time is shown, as well as the arithmetic average wind magnitude and wind direction. The most striking feature is the strong wind speed along the East Greenland ice edge. Note that only grid points which are ice-free at least 25 % of the time are included in the plot. Because it is difficult to represent the winds near the variable ice edge in a coherent manner, the average wind speed relative to the edge of the sea-ice is presented and discussed in the next section.

The average wind field follows a distinct seasonal cycle. From November to March, when the synoptic activity is high, the winds in the Greenland Sea predominantly come from the north, leading to a high frequency of marine cold-air outbreaks on the northeastern flanks of synoptic lows.

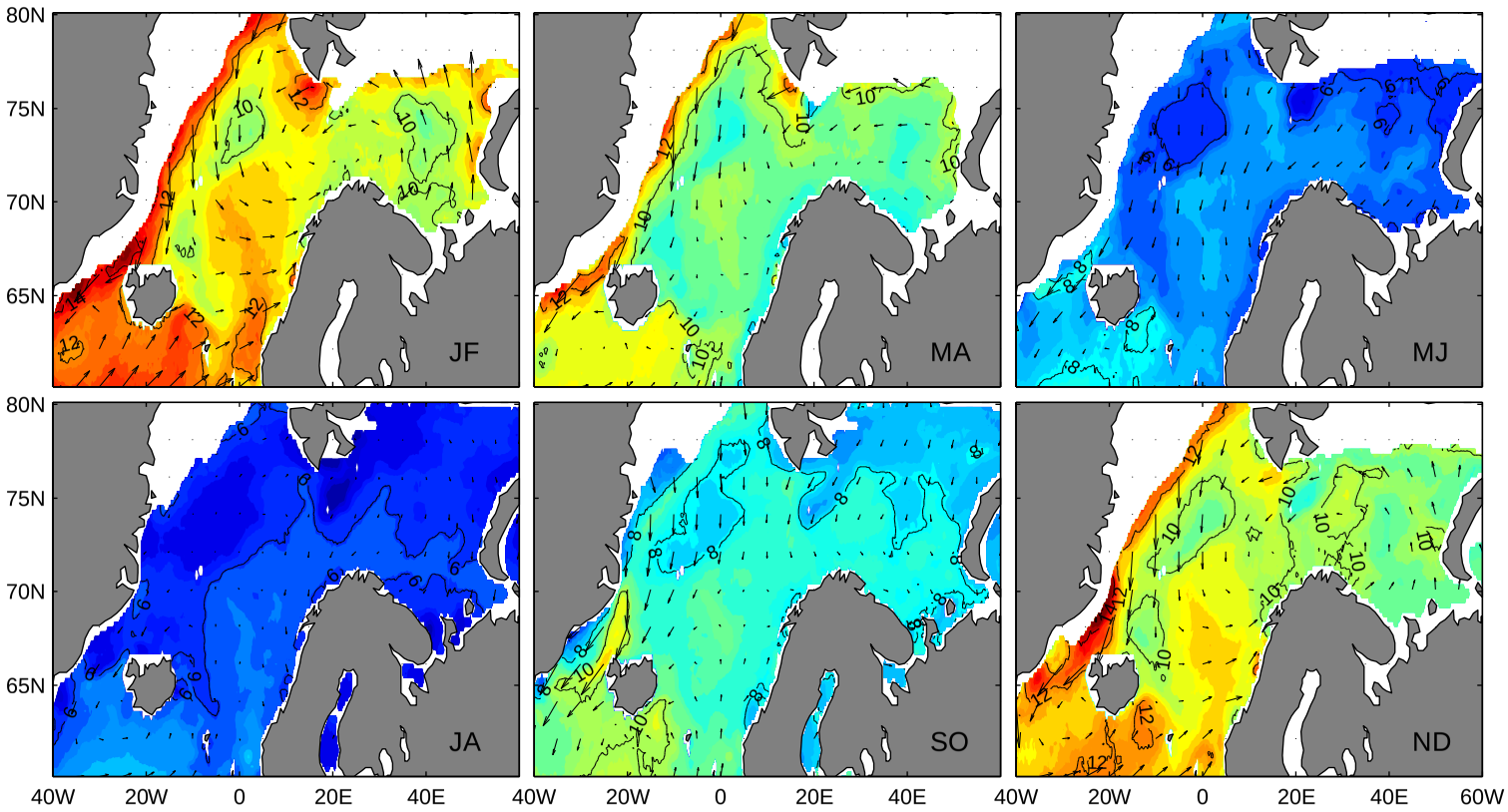

Figure 3: Average QuikSCAT surface wind speed (in ms^{-1} inside filled contours) and arithmetic mean wind vectors (arrows; longest arrow is 7.9 ms^{-1} in November–December) for two months at a time. Grid cells where there is ice more than 75 % of the time are not shown.

The wind shadow to the north and northeast of Iceland is consistent with the findings of Kristjansson and McInnes (1999). They found that lows travelling through the Denmark Strait from the southwest were influenced by the topography of Greenland. The baroclinic development of the cyclone was suppressed, and a secondary, quasi-stationary low was formed south of the Denmark Strait as the weakened low progressed into the Greenland Sea. The climatological importance of this lee effect is supported by subsequent studies (Petersen et al., 2003; Schwierz and Davies, 2003).

South of Iceland, January and February are the windiest months. An interesting feature is that during these months the position of the Icelandic low seems to be further to the southwest than in November–December and March–April, but with only 7-8 years of data, this difference is not necessarily significant.

The strong winds just north of Iceland (at their "Denmark Strait North" location) were suggested by Moore and Renfrew (2005) to be due to a combination of barrier winds to the left of the Greenland coast, a rightward bending and convergence enforced by the topography of Iceland and katabatic winds. The late autumn barrier winds, when there is yet little ice near the coastline, are clearly connected to topography. The orography-induced pressure gradients along the coast clearly bend the northerly winds towards the right. In addition, channelling effects create a tongue of high wind speed through the Denmark Strait. In the summer, when there is no persistent northerly component to the wind, this effect is not as clear as throughout the rest of the year. During winter, the ice edge stretches further from the coastline, and small-scale baroclinic air-sea interactions in the marginal ice zone are likely to amplify the effect of the barrier winds in the Denmark Strait.

Further north, the surface jet near the southern tip of Spitsbergen, as described by Skeie and Grønås (2000) can be seen, especially during the winter months when the average wind is from the northeast. The high wind speeds downstream of the northern tip of Spitsbergen are probably linked to the tip jet that was analysed by Sandvik and Furevik (2002) as well as interactions with the sea-ice. In agreement with Skeie and Grønås (2000), there are indications of a wake between the two jets directly west of Spitsbergen. It seems likely that the wind speed minimum to the northeast of Jan Mayen is due to a combination of the impact of Greenland discussed above and the Spitsbergen wake. Between Hopen and

Bjørnøya (to the south of the main fjord on the southeastern part of Spitsbergen, Storfjorden), another interesting wind speed nadir is found during the months with a high frequency of northeasterly winds. This is most likely tied to the shallow water under the "Bear Island ice tongue" described by (Nghiem et al., 2005), although it is not clear how. Errors due to undetected sea-ice can not be ruled out.

The average circulation seems to be centered to the south of Bjørnøya. This can be interpreted as a thermal low (or in fact a constant sea breeze, as the diurnal cycle is very weak during winter because of low insolation) when the temperature difference between the open water and the air over the ice is at its largest (roughly from November to February, again because of low insolation). Wu et al. (2004) found negative SLP anomalies over the Greenland and Barents Seas during winters with little sea-ice, and suggested that this was a positive feedback mechanism on the ice extent. Similar conclusions were reached by Bengtsson et al. (2004), who proposed that increased cyclogenesis in the Barents Sea during years with little sea-ice produces winds that drive the ice northwards.

There is a distinct wind shadow behind Northern Scandinavia and the Kola peninsula, and especially in January–February. A possible explanation for this is that synoptic lows are retarded as they move into the Barents Sea; Hoskins and Hodges (2002) found that storms moving northeastwards along the Northeast Atlantic storm track slowed down over the Norwegian Sea. Another possibility is that the southwesterly winds are weakened by frictional effects as they move over land on their way to the Barents Sea.

January is the windiest month in the Barents Sea, especially in the northeastern part. A southerly surface jet is found along the west coast of Novaya Zemlya, most likely because the average wind is a strong southerly in this month. It is also interesting to note that the winds are marginally weaker in February than in both January and March (not shown specifically). A nadir in polar low activity has been found by independent sources (Lystad, 1986; Noer and Ovhed, 2003; Kolstad, 2006), and it has been speculated that it is due to a higher frequency of blocking highs over Scandinavia and lower synoptic activity in that month. In Figure 3, there is no evidence of anticyclonic circulation, but the average Barents Sea winds turn from weak southerlies in February to moderately strong northeasterlies in March near the northern ice edge (not shown). This leads to a weakening of

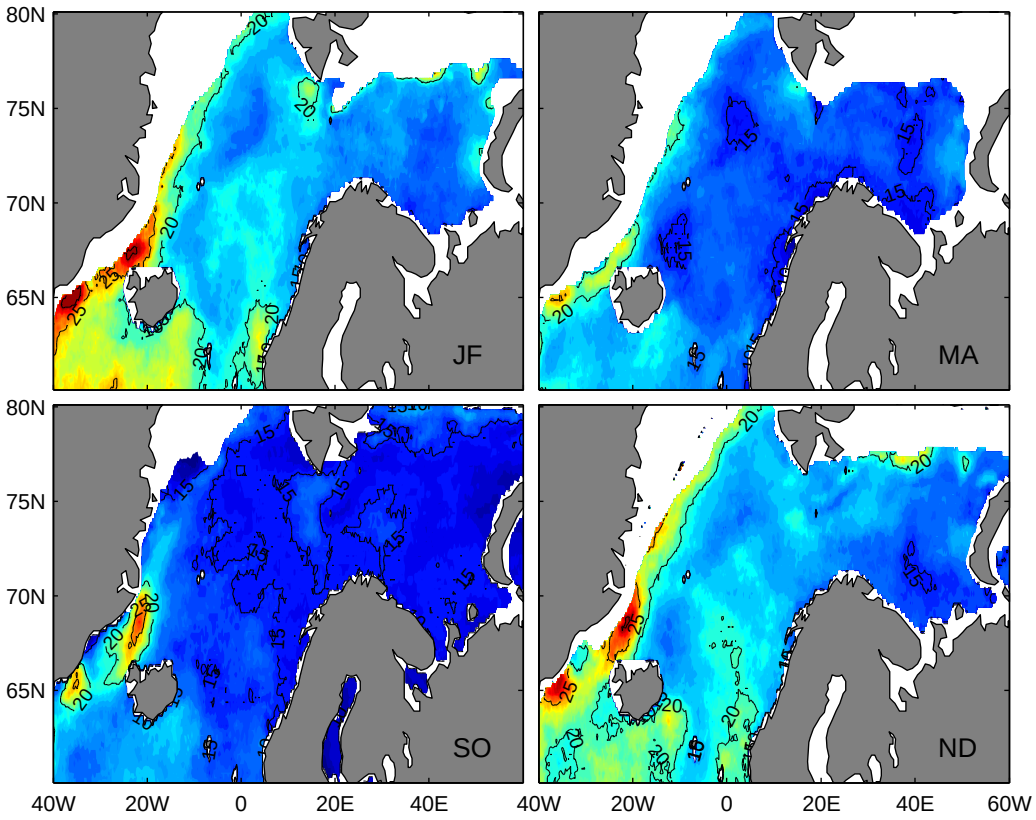

Figure 4: As Figure 3, but the 0.95 quantile values of wind speed (in ms^{-1}).

the wind field near Novaya Zemlya and a strengthening in the north (possibly because of a higher frequency of cold-air outbreaks) in March. Further west, over the Norwegian and Greenland Seas, the winds are stronger in February than in March, including the orographic jet near the southern tip of Spitsbergen (possibly because the air masses over the ice sheet east of Spitsbergen are strongly stable because there is no sun).

4.2 Extreme winds

The 0.95 wind speed quantile values are shown in Figure 4. With two samples per day a 0.95 quantile value is exceeded on average roughly 3 times per month.

The largest quantile values by far are found in the “Denmark Strait North” and

"Denmark Strait South" locations (Moore and Renfrew, 2005), where the 0.95 quantile of the wind speed exceeds 30 ms^{-1} in winter and 25 ms^{-1} in autumn. It is noteworthy that the values there are substantially larger than the ones found over the open ocean to the south of Iceland. While it is obvious that the topography is the main cause of these exceptionally high values, it is possible that interactions with the ice edge are important in January–February. During these months, the northern maximum migrates slightly towards the south, while the southern maximum remains fixed.

Over the Barents Sea, high values are found near the ice edge in winter, especially in the region around 40°E. The surface jet by the southern tip of Spitsbergen gives high values in January–February, but this location does not stand out as much as it did with respect to the mean winds. A possible interpretation is that the jet is fairly persistent, but that severe winds occur rather infrequently. A similar argument can be applied to the topographically forced southerly jet outside the coast of Western Norway, although high values are found throughout the winter and seem to penetrate far north into the Norwegian Sea.

4.3 Wind speed relative to the ice edge

A typical case with strong northerly winds along the East Greenland ice edge is shown in Figure 5, a satellite image taken on 28 April 2002. Figure 6 is a comparison between QuikSCAT and NCEP-R 10-metre surface winds on the same day. The QuikSCAT data are only valid over open water, and the wind-torn sea-ice near the edge of the ice sheet is deleted. The winds are much stronger than their NCEP-R counterparts, probably due to a combination of katabatic effects and frontal features near the ice edge. The hurricane-force winds at the entrance to the Denmark Strait are forced by orography as described by Moore and Renfrew (2005). There is also a wind speed maximum just east of location A, which might be an error because of undetected sea-ice, but could also be due to small-scale wind channelling through one of the fjords. Far from the ice edge, the two data sources agree about the wind speed, but in the marginal ice zone, subgrid-scale processes take over, and the NCEP-R assimilating model does not have the necessary horizontal resolution to reproduce these features.

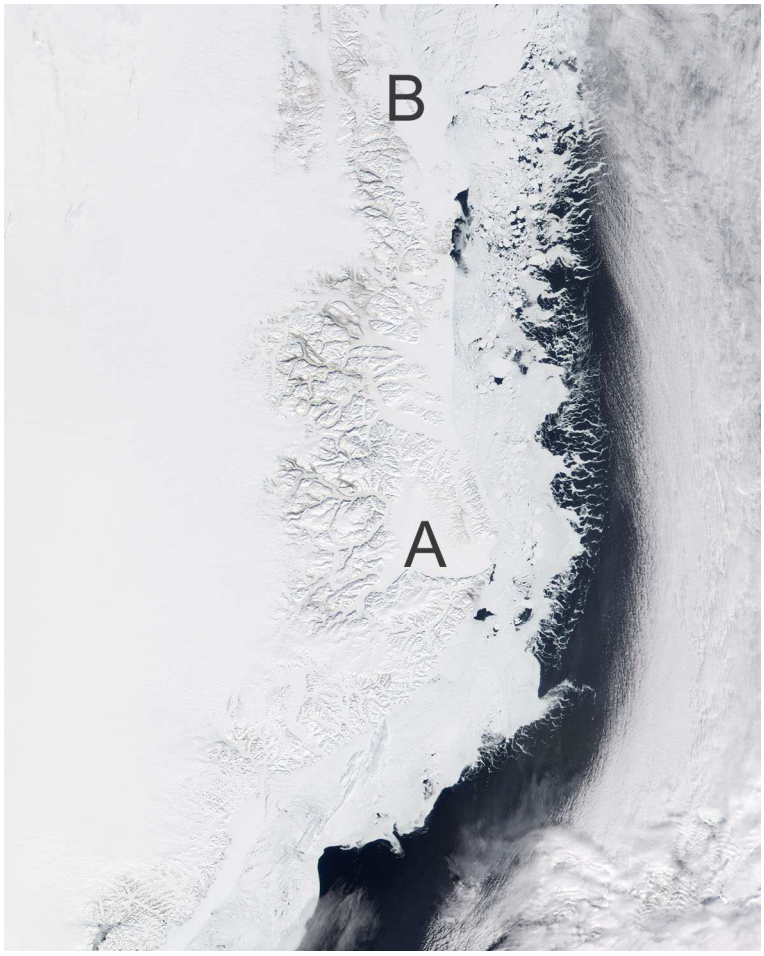

Figure 5: A satellite image (courtesy of NASA's Visible Earth programme) of the east coast of Greenland on 28 April 2002. The locations A and B match those in Figure 6.

The 0.95 quantile of the wind speed relative to the ice edge along the east coast of Greenland is shown in Figure 7. Note that there is some 'noise' in the upper right corners of some of the plots because of the location of Spitsbergen. The summer months were left out due to low quantile values.

Overall, the extreme values of the wind speed in a narrow band along the ice edge are exceptionally high. Just south of 74°N, the quantile values are higher than 25 ms^{-1} in November–December. These values are only slightly lower than the ones found north of the Denmark Strait (Figure 4).

There is a distinct maximum just south of 74°N. This location coincides with

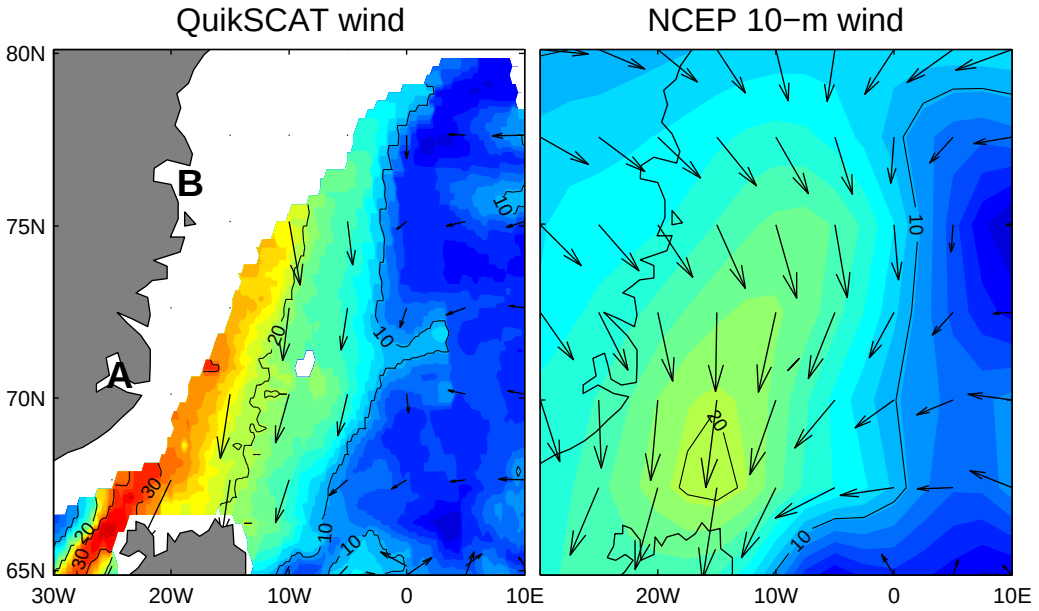

Figure 6: QuikSCAT surface wind and NCEP-R 10-metre wind on the morning (0600 UTC for NCEP-R) of 28 April 2002. The locations A and B match those in Figure 5.

the location of the "Odden" feature, a tongue of sea-ice which forms irregularly between latitudes 70°N and 74°N (Shuchman et al., 1998; Comiso et al., 2001; Wilkinson, 2006). It is possible that the strong winds are linked to this phenomenon. Shuchman et al. (1998) analysed meteorological observations at times when Odden was formed and found that relatively weak westerly winds and very low air temperatures were favourable for Odden formation, while strong northerlies were found to break up the feature. It is not clear how the extreme winds in this region influence Odden (or the other way around), but it seems likely that they contribute to the observed rapid variability of the feature. Perhaps a topographical feature leads to a high frequency of channelling or katabatic effects, which again lead to large heat fluxes from the ocean and rapid freezing.

North of 78°N another region with high quantile values is found. This is near the entrance to the Fram Strait, where sea-ice is exported from the Arctic Ocean to the Atlantic. It is possible that the strong winds in this area are connected to the wind direction.

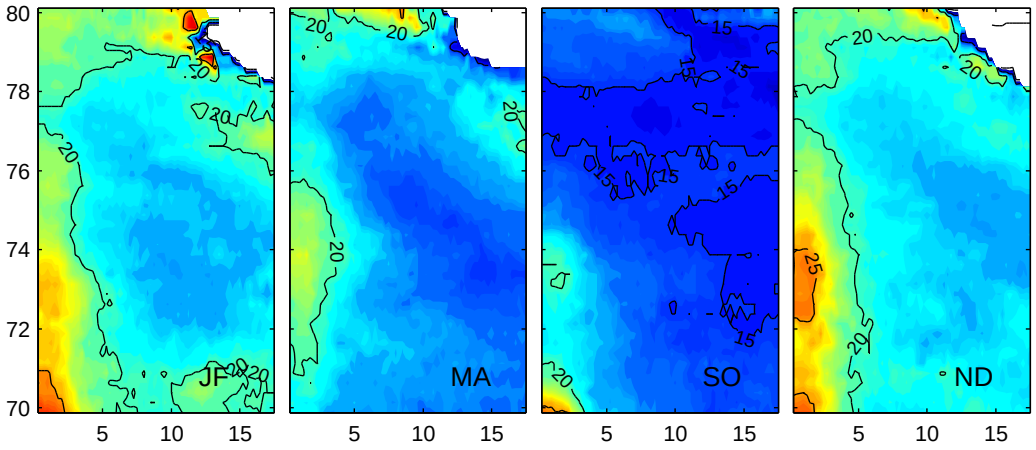

Figure 7: QuikSCAT wind speed 0.95 quantile values (in ms^{-1}) in the grid cells to the immediate east of the ice edge or the coastline of eastern Greenland. The ice edge or the coast is to the left, and the latitude (longitude relative to the edge) is marked on the y-axes (x-axes). The vertical distance is 1110 km, and the horizontal distance is 670 km at the bottom and 340 km at the top. Note that in a non-stationary coordinate system such as this one, it does not make sense to plot the wind vectors.

In Figure 8 the average wind direction (in terms of U and V) at the first valid QuikSCAT grid point from the west is shown. During summer there is no preferred wind direction, but throughout the rest of the year, the V-component of the wind at the ice edge is distinctly negative. Assuming that the ice edge is directed towards north-northeast from south-southwest, the wind is parallel to the ice edge when both V and U are negative. In such conditions, under the assumption that the thermal wind direction is parallel to the ice edge towards north-northeast, the actual wind has the opposite direction. This configuration is called reverse-shear flow (Duncan, 1978), and is favourable for strong surface winds and enhanced air-sea interaction in the form of large heat fluxes from the ocean to the atmosphere.

Several Arctic fronts in reverse-shear conditions have been studied in the literature (Shapiro and Fedor, 1989; Thompson and Burk, 1991; Økland, 1998; Grønås and Skeie, 1999; Drue and Heinemann, 2001), and a substantial wind shear was common to all of them. Strong wind speeds were found near the ice edge over open water, and large heat fluxes were either observed or simulated. The aver-

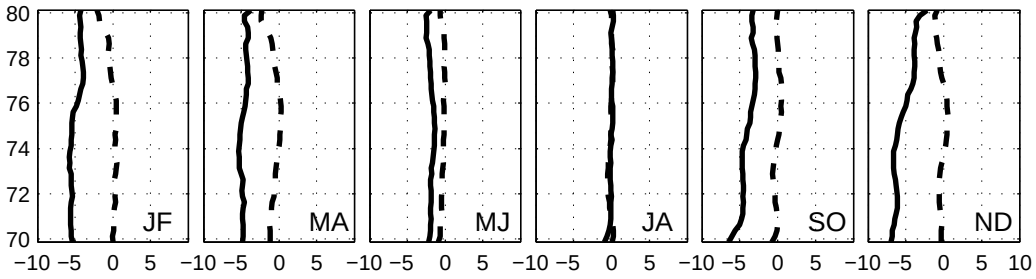

Figure 8: Average QuikSCAT wind components at the ice edge. Latitudes are shown on the y-axes, and the U-component is drawn with a dashed line (values on the x-axes in ms^{-1}). The V-component is drawn with a solid line.

age wintertime wind north of 78°N and, although this is a weaker signal, around the wind speed maxima near 74°N, are both directed along the ice edge, and it is possible that this is the reason for the high winds speeds observed there. Between these two locations the winds speeds are lower, possible because the wind is directed out from the ice sheet rather than parallel to it.

The winds in the marginal ice zone in the Barents Sea are not as strong as the ones in the Greenland Sea (possibly due to the lack of persistent reverse-shear conditions), and are not discussed here.

4.4 Comparison with NCEP reanalysis

The high level of detail in the QuikSCAT data is not available in synoptic analyses such as the NCEP reanalysis or the ERA-40 project. These data sets are, as it were, a compromise between assimilation of observations and the dynamical consistency required by the underlying numerical model. To first order, they may be regarded as the synoptic background forcing field, and the difference between the reanalyses and the observations is due to sub-grid, mesoscale effects or low-resolution topography.

In Figure 9 the difference between QuikSCAT and NCEP-R surface winds is shown. The NCEP-R 10-metre wind field was interpolated onto the QuikSCAT grid using a nearest-neighbour approach, and invalid QuikSCAT pixels (due to either sea-ice cover or rain) were deleted for consistency (as in Figure 3). The

NCEP-R winds alone are shown in Figure 10.

Over open ocean the NCEP-R winds are too strong. The wind shadow to the north of Iceland is not as pronounced in NCEP-R as in QuikSCAT. A very likely explanation for this is that the coarse representation of topography in NCEP-R prohibits the lee cyclogenesis south of the Denmark Strait as described by Kristjansson and McInnes (1999). The overestimation of the Greenland Sea wind speed is particularly large during winter, when the synoptic activity in the region is high. The underestimation of the winds to the southwest of Iceland during these months supports the conjecture that coarse topography is to blame (because of the apparent lack of a residual low in that region).

Topography issues most likely also explain why the barrier winds in the Denmark Strait are too strong in NCEP-R in the summer and autumn. In the plot for September–October in Figure 3, there is a pronounced wake where the positive bias is seen in the corresponding plot in Figure 9. Similarly, the positive wind speed bias in the Barents Sea, where a wind shadow was seen in Figure 3, could also be due to a poor representation of topography in NCEP-R. Another point of interest is that the NCEP-R winds are stronger then QuikSCAT over the shallow water of the Svalbard Bank, which might be due to a QuikSCAT bias because of undetected sea-ice.

Furthermore, the NCEP-R winds are too strong over the open Nordic Seas in general, including their southerly component along the coast of Northern Norway, suggesting that the synoptic activity is too strong in the central Norwegian Sea. The lack of data in sparsely inhabited regions is probably the main reason for the NCEP-R bias. Condron et al. (2006) investigated the ability of ERA-40 to represent mesoscale cyclones in the Northeast Atlantic, and found that the correctly identified cyclones were generally clustered around synoptic observing stations.

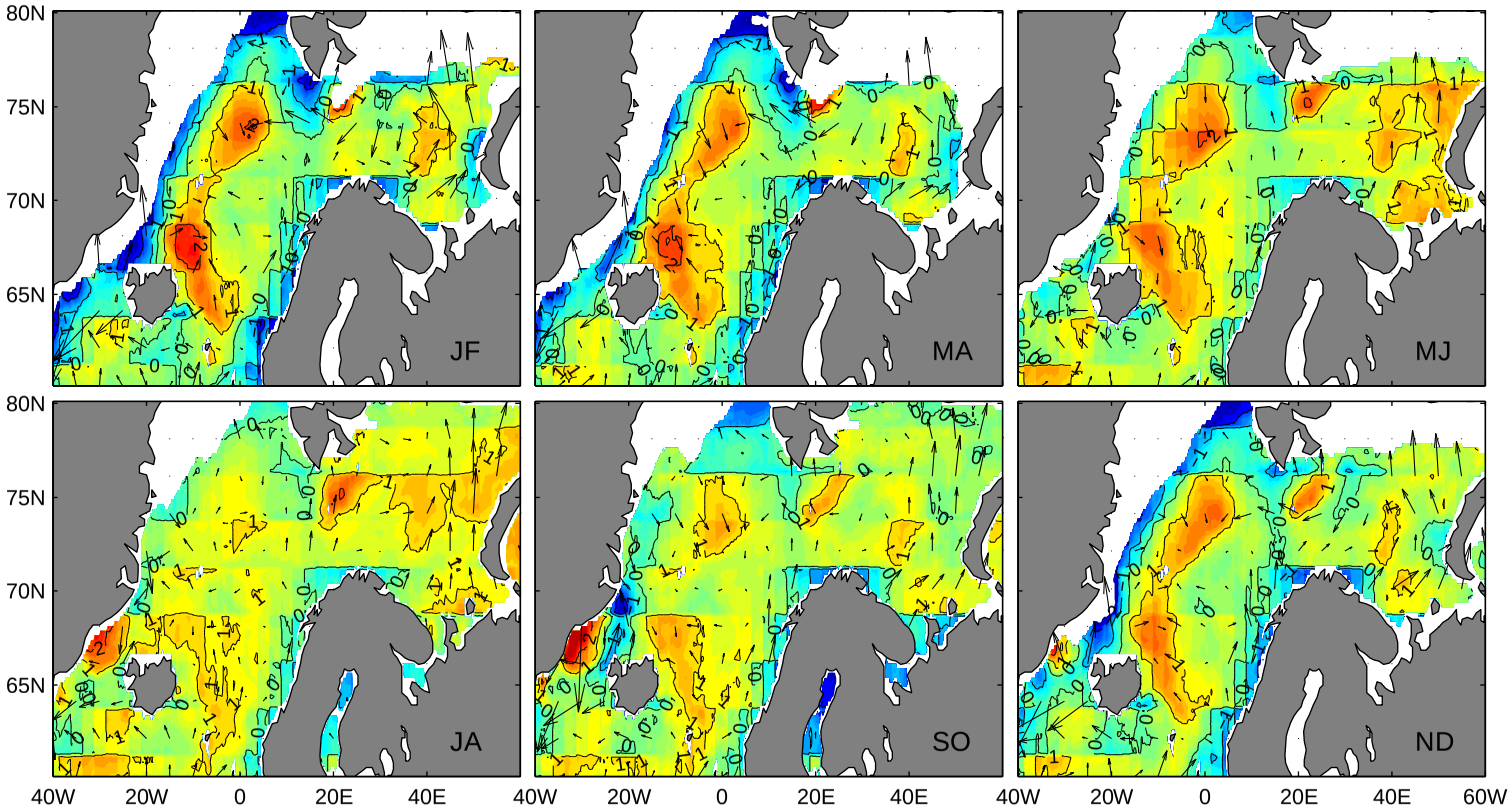

Figure 9: The difference between NCEP-R and QuikSCAT wind speed (contours) and arithmetic mean wind vectors (arrows). The scale of the arrows is not the same as in Figure 3, and the longest arrow corresponds to 4.4 ms^{-1} in November–December.

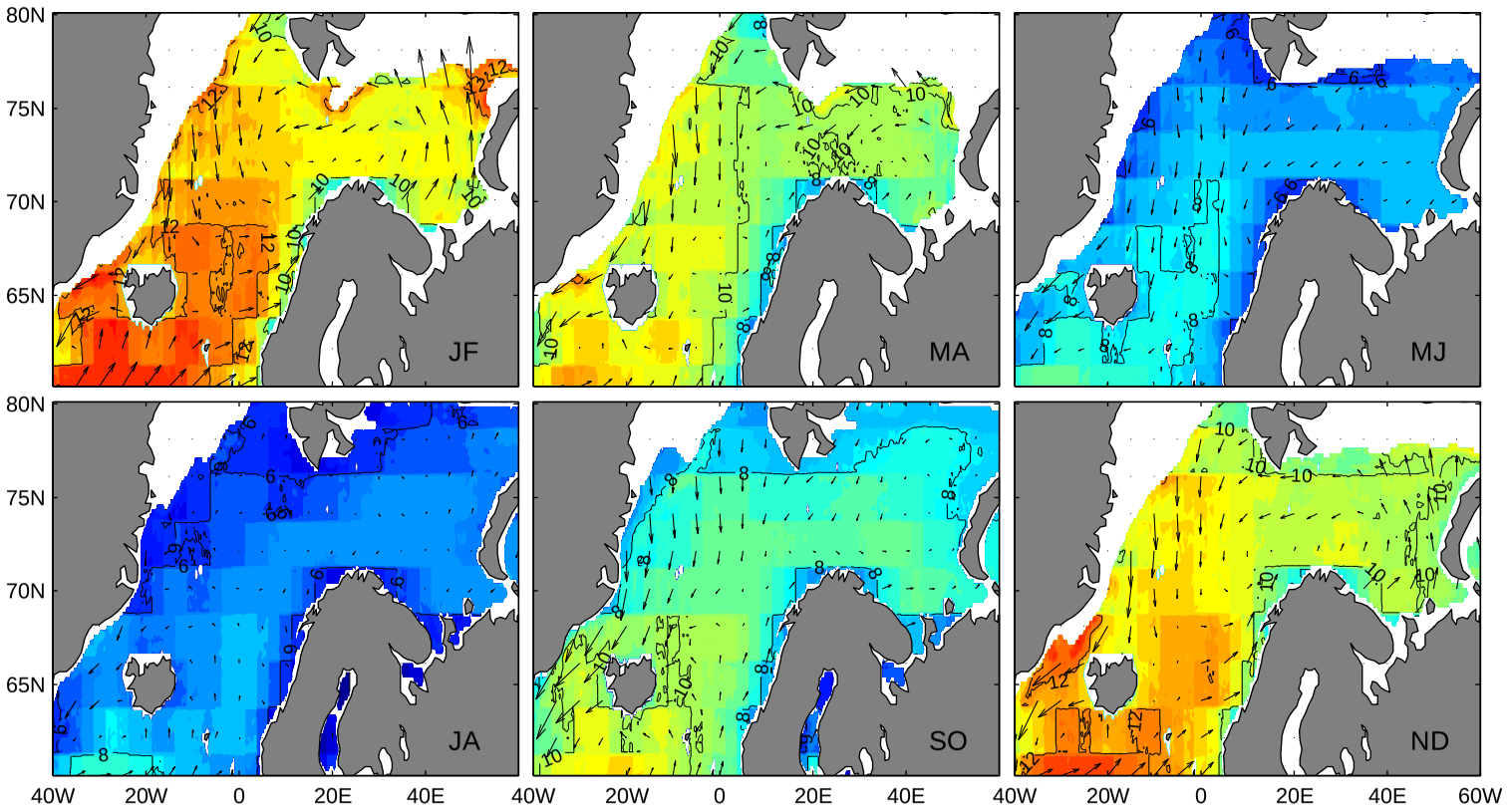

Figure 10: As Figure 3, but for NCEP-R 10-metre wind interpolated onto the QuikSCAT grid (hence the jagged contours). The scale of the arrows is the same as in Figure 3, and the longest arrow corresponds to 8.5 ms^{-1} in January–February.

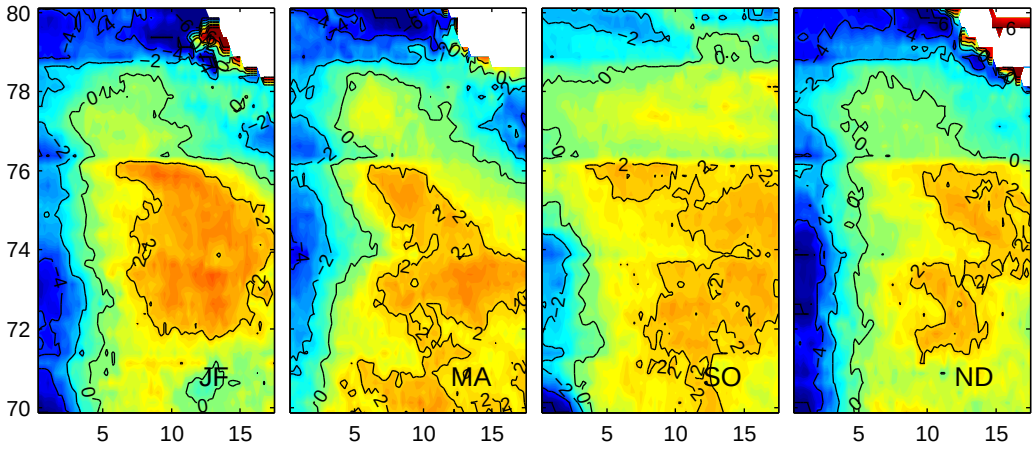

Figure 11: The difference between NCEP-R and QuikSCAT 0.95 wind speed quantile values. The coordinate system is the same as in Figure 7.

The difference between the NCEP reanalysis and QuikSCAT 0.95 wind speed quantile values in a coordinate system relative to the sea-ice edge is shown in Figure 11. The wind speed along the ice edge is clearly underestimated by NCEP-R. One possible, and likely, interpretation of the differences is that the strong QuikSCAT winds are a 'residual' due to air-sea interactions which are on a subgrid-scale in NCEP-R. The low horizontal resolution of NCEP-R makes it impossible to represent small-scale processes in the shallow boundary layer in the marginal ice zone. Indeed, even high-resolution numerical models are sometimes unable to properly reproduce features such as polar lows (Pagowski and Moore, 2001). Liu et al. (2006) found that a horizontal resolution of 0.5 km (and down to 25 m in the vertical) was needed to fully simulate roll clouds in a marine cold-air outbreak. Obviously, NCEP-R can not be expected to take such features into account. The QuikSCAT data is the only data source to provide an observational record which is long enough to allow quantification of the long-term importance of the winds near the ice edge.

5 Summary and discussion

In this paper high-resolution satellite-derived wind data was used to provide a climatology of both average and extreme winds in the Nordic Seas. A number of localised phenomena were identified, such as the persistent strong northerly winds in the Denmark Strait, coupled with a wake region downstream of the elevated topography, a southerly jet along the coast of Western Norway, a jet near the southern tip of Spitsbergen, a wake region to the southwest of Spitsbergen, a wind shadow to the northeast of Iceland and over the Barents Sea to the northeast of Northern Scandinavia and the Kola peninsula.

In addition to these features, a substantial localised strengthening of the winds near the sea-ice edge along the east coast of Greenland was found. It was suggested that the strongest winds occur in locations where the average wind field corresponds to reverse shear, i.e. the wind is directed along the ice edge with the cold air to its right, in the opposite direction of the thermal wind. In the words of Duncan (1978): "A reversed shear flow will usually, although not necessarily, have a greater vertical wind shear in the boundary layer than the more normal flow. This implies an enhancement of the surface fluxes of momentum, heat and moisture."

In view of previous literature on air-sea interactions in the marginal ice zone the strong winds are perhaps not surprising, but the magnitude of the differences with respect to NCEP reanalysis data is exceptionally large. It is important to quantify these differences, as well as the strong winds in themselves, for many reasons, e.g.:

1) Navigation: Økland (1998) attributed a tragic accident in the Greenland Sea in 1952, when 78 lives were lost in a storm, to a reverse-shear cold-air outbreak from the ice sheet. Such conditions represent a double hazard, as the wind will pack drifting ice towards the solid ice edge, and Arctic fronts may develop at the leading edge of the cold air. Numerical simulations performed at the Geophysical Institute in Bergen have shown that an Arctic front was present in the vicinity when the British trawler Gaul went down in the Norwegian Sea in 1974. A quantification of the regional likelihood of strong winds is a potentially powerful tool for navigational purposes.

2) Forecasting: It is important for weather forecasters to be aware of when, where and under which conditions strong winds are likely to occur. In addition, Chelton et al. (2006) have shown that direct assimilation of QuikSCAT winds may improve numerical forecasts considerably.

3) Oceanography: Ocean models are routinely forced with atmospheric reanalysis products such as NCEP-R and ERA-40 (e.g. Haak et al., 2003). Momentum is transferred from the atmosphere to the ocean by the wind stress, defined as $T = \rho C_D U_{10}^2$. A 10-metre wind speed of 15 ms^{-1} thus yields a wind stress which is 2.25 times larger than the stress of a 10 ms^{-1} surface wind. Incorrect wind speeds may introduce unwanted model biases. This is especially true for individual case with high wind speeds; Morey et al. (2005) used QuikSCAT winds to simulate the circulation driven by mesoscale atmospheric forcing and concluded that satellite-derived winds showed "great promise for representing energetic episodic events such as tropical cyclones". The discovery of the Greenland tip jet (Doyle and Shapiro, 1999; Moore and Renfrew, 2005) lead Pickart et al. (2003) to force an ocean model with a number of tip jet events. They found that deep convection took place, and claimed that the tip jet was "the most likely cause of the convection in the Irminger Sea". It is not unlikely that a model forced with QuikSCAT winds in the exceptionally windy Greenland Sea marginal ice zone will provide new insight into the properties of the cold East Greenland Current and the corresponding transport of both freshwater and sea-ice.

4) Sea-ice movement: In a modelling experiment, Harder et al. (1998) found that the sea-ice export through the Fram Strait had a roughly linear dependence on the wind speed over the ice. The effect of ocean currents was found to be much weaker. On a more local scale, Brummer et al. (2003) investigated the impact on the sea-ice movement in the marginal ice zone of a weakening cyclone moving northwards into the Fram Strait. They found that the passage of the cyclone had a significant influence on both the speed and direction of the sea-ice drift. Large-scale, low-frequency atmospheric patterns have also been shown to influence the sea-ice movement, most recently by Wu et al. (2006). They found that the second EOF of sea level pressure north of 70°N corresponded to a dipole of pressure with centers over northern Eurasia and over northern Canada and Greenland. A similar dipole was found by Skeie (2000). In the positive phase of what he called the

"Barents Oscillation", anomalously strong northerly winds prevail, and the export of sea-ice through the Fram Strait is enhanced. It is not unlikely that small-scale processes which take place in such conditions contribute (sometimes invisibly) to the larger picture.

5) Dynamical insight: The evidence of frequent strong winds in the marginal ice zone should highlights the need for in-situ observations. While Arctic fronts have been the subject of a few observational campaigns (Shapiro and Fedor, 1989; Drue and Heinemann, 2001), much stands to be gained from further field work. Perhaps the most interesting parameter is the heat flux between the sea and the boundary layer. At present, it is not clear how strong the fluxes can get in extreme conditions, and there is a need for reliable observational data. In addition to heat flux measurements, a thorough mapping of the synoptic conditions and background flow, the structure of the sea-ice near its edge, the spatial structure of the temperature of the sea surface, the depth of the ocean mixed layer, the wave height and wavelength, the depth of the atmospheric boundary layer are all fields and parameters that should be taken into account in a large-scale field experiment. Such insight might also directly improve the accuracy of numerical models. Pagowski and Moore (2001) have shown that even high-resolution, non-hydrostatic numerical models were unable to properly reproduce a polar low in a marine cold-air outbreak. In their own words: "The default surface-layer parameterisation included in the model is shown to grossly overestimate the magnitude of the air-sea interaction resulting in forecasts of boundary layer growth and mesoscale development that differ substantially from observations."

References

Barstad, I. and S. Grønås, 2005: Southwesterly flows over southern Norway - mesoscale sensitivity to large-scale wind direction and speed. *Tellus*, **57A**, 136–152.

Bengtsson, L., V. A. Semenov and O. M. Johannessen, 2004: The early twentieth-century warming in the Arctic - A possible mechanism. *Journal Of Climate*, **17**, 4045–4057.

Blindheim, J. and S. Østerhus, 2005: The Nordic Seas, Main Oceanographic Fea-

tures. In *The Nordic Seas: An Integrated Perspective*, 11–37. American Geophysical Union.

Bresch, J. F., R. J. Reed and M. D. Albright, 1997: A polar-low development over the Bering Sea: Analysis, numerical simulation, and sensitivity experiments. *Monthly Weather Review*, **125**, 3109–3130.

Brummer, B., G. Muller and H. Hoeber, 2003: A Fram Strait cyclone: Properties and impact on ice drift as measured by aircraft and buoys. *Journal Of Geophysical Research-Atmospheres*, **108**.

Chelton, D., M. Freilich, J. Sienkiewicz and J. Von Ahn, 2006: On the use of QuikSCAT scatterometer measurements of surface winds for marine weather prediction. *Monthly Weather Review*, **134**, 2055–2071.

Comiso, J. C., P. Wadhams, L. T. Pedersen and R. A. Gersten, 2001: Seasonal and interannual variability of the Odden ice tongue and a study of environmental effects. *Journal Of Geophysical Research-Oceans*, **106**, 9093–9116.

Condron, A., G. R. Bigg and I. A. Renfrew, 2006: Polar mesoscale cyclones in the northeast Atlantic: Comparing climatologies from ERA-40 and satellite imagery. *Monthly Weather Review*, **134**, 1518–1533.

Doyle, J. and M. Shapiro, 1999: Flow response to large-scale topography: the Greenland tip jet. *Tellus*, **51A**, 728–748.

Drue, C. and G. Heinemann, 2001: Airborne investigation of arctic boundary-layer fronts over the marginal ice zone of the Davis Strait. *Boundary-Layer Meteorology*, **101**, 261–292.

Drue, C. and G. Heinemann, 2002: Turbulence structures over the marginal ice zone under flow parallel to the ice edge: Measurements and parameterizations. *Boundary-Layer Meteorology*, **102**, 83–116.

Duncan, C., 1978: Baroclinic Instability In A Reversed Shear-Flow. *Meteorological Magazine*, **107**, 17–23.

Furevik, T. and J. E. Ø. Nilsen, 2005: Large-Scale Atmospheric Circulation Variability and Its Impacts on the Nordic Seas Ocean Climate-A Review. In *The Nordic Seas: An Integrated Perspective*, 105–136. American Geophysical Union.

Grønås, S. and P. Skeie, 1999: A case study of strong winds at an Arctic front. *Tellus*, **51A**, 865–879.

Haak, H., J. Jungclaus, U. Mikolajewicz and M. Latif, 2003: Formation and propagation of great salinity anomalies. *Geophysical Research Letters*, **30**.

Harder, M., P. Lemke and M. Hilmer, 1998: Simulation of sea ice transport through Fram Strait: Natural variability and sensitivity to forcing. *Journal Of Geophysical Research-Oceans*, **103**, 5595–5606.

Harold, J. M., G. R. Bigg and J. Turner, 1999a: Mesocyclone activity over the North-East Atlantic. Part 1: Vortex distribution and variability. *International Journal Of Climatology*, **19**, 1187–1204.

Harold, J. M., G. R. Bigg and J. Turner, 1999b: Mesocyclone activity over the Northeast Atlantic. Part 2: An investigation of causal mechanisms. *International Journal Of Climatology*, **19**, 1283–1299.

Hoffman, R. N. and S. M. Leidner, 2005: An introduction to the near-real-time QuikSCAT data. *Weather And Forecasting*, **20**, 476–493.

Hoskins, B. and K. Hodges, 2002: New perspectives on the Northern Hemisphere winter storm tracks. *Journal Of The Atmospheric Sciences*, **59**, 1041–1061.

Hurrell, J. W., M. Visbeck, A. Busalacchi, R. A. Clarke, T. L. Delworth, R. R. Dickson, W. E. Johns, K. P. Koltermann, Y. Kushnir, D. Marshall, C. Mauritzen, M. S. McCartney, A. Piola, C. Reason, G. Reverdin, F. Schott, R. Sutton, I. Wainer and D. Wright, 2006: Atlantic climate variability and predictability: A CLIVAR perspective. *Journal Of Climate*, **19**, 5100–5121.

Kållberg, P., A. Simmons, S. Uppala and M. Fuentes, 2004: The ERA-40 archive. *ERA-40 Project Report Series*, **17**, 31.

Kalnay, E., M. Kanamitsu, R. Kistler, W. Collins, D. Deaven, L. Gandin, M. Iredell, S. Saha, G. White, J. Woollen, Y. Zhu, M. Chelliah, W. Ebisuzaki, W. Higgins, J. Janowiak, K. Mo, C. Ropelewski, J. Wang, A. Leetmaa, R. Reynolds, R. Jenne and D. Joseph, 1996: The NCEP/NCAR 40-year reanalysis project. *Bulletin Of The American Meteorological Society*, **77**, 437–471.

Klein, T. and G. Heinemann, 2002: Interaction of katabatic winds and mesocyclones near the eastern coast of Greenland. *Meteorological Applications*, **9**, 407–422.

Kolstad, E., 2006: A new climatology of favourable conditions for reverse-shear polar lows. *Tellus*, **58A**, 344–354.

Kristjansson, J. E. and H. McInnes, 1999: The impact of Greenland on cyclone evolution in the North Atlantic. *Quarterly Journal Of The Royal Meteorological Society*, **125**, 2819–2834.

Lamb, H., 1991: Cambridge University Press, Cambridge.

Leslie, L. M. and B. W. Buckley, 2006: Comments on Scatterometer-based assessment of 10-m wind analyses from the operational ECMWF and NCEP numerical weather prediction models.. *Monthly Weather Review*, **134**, 737–742.

Liu, A., G. Moore, K. Tsuboki and I. Renfrew, 2006: The effect of the sea-ice zone on the development of boundary-layer roll clouds during cold air outbreaks. *Boundary-Layer Meteorology*, **118**, 557–581.

Lystad, M., 1986: Polar lows project; Final report: polar lows in the Norwegian, Greenland and Barents Sea.

Moore, G. and I. Renfrew, 2005: Tip jets and barrier winds: A QuikSCAT climatology of high wind speed events around Greenland. *Journal of Climate*, **18**, 3713–3725.

Morey, S. L., M. A. Bourassa, X. J. J. Davis, J. J. O'Brien and J. Zavala-Hidalgo, 2005: Remotely sensed winds for episodic forcing of ocean models. *Journal Of Geophysical Research-Oceans*, **110**, C10024.

Nghiem, S., M. Van Woert and G. Neumann, 2005: Rapid formation of a sea ice barrier east of Svalbard. *Journal Of Geophysical Research-Oceans*, **110**.

Noer, G. and M. Ovhed, 2003: Forecasting of polar lows in the Norwegian and the Barents Sea. In *9th meeting of the EGS Polar Lows Working Group*. Cambridge, UK.

Økland, H., 1998: Modification of frontal circulations by surface heat flux. *Tellus*, **50A**, 211–218.

Pagowski, M. and G. Moore, 2001: A numerical study of an extreme cold-air outbreak over the Labrador Sea: Sea ice, air-sea interaction, and development of polar lows. *Monthly Weather Review*, **129**, 47–72.

Petersen, G. N., H. Olafsson and J. E. Kristjansson, 2003: Flow in the lee of idealized mountains and Greenland. *Journal Of The Atmospheric Sciences*, **60**, 2183–2195.

Pickart, R. S., M. A. Spall, M. H. Ribergaard, G. W. K. Moore and R. F. Milliff, 2003: Deep convection in the Irminger Sea forced by the Greenland tip jet. *Nature*, **424**, 152–156.

Rasmussen, E. and J. Turner, 2003: *Polar Lows*. Cambridge University Press, Cambridge.

Rogers, J., 1997: North Atlantic storm track variability and its association to the north Atlantic oscillation and climate variability of northern Europe. *Journal of Climate*, **10**, 1635–1647.

Sandvik, A. and B. Furevik, 2002: Case study of a coastal jet at Spitsbergen - Comparison of SAR- and model-estimated wind. *Monthly Weather Review*, **130**, 1040–1051.

Schwierz, C. B. and H. C. Davies, 2003: Evolution of a synoptic-scale vortex advecting toward a high mountain. *Tellus*, **55A**, 158–172.

Shapiro, M. and L. Fedor, 1989: A case study of an ice edge boundary layer front and polar low development over the Norwegian and Barents Seas. In *Polar and Arctic Lows*, 279–89. A Deepak, Hampton, VA.

Shapiro, M., T. Hampel and L. Fedor, 1989: Research aircraft observations of an arctic front over the Barents Seas. In *Polar and Arctic Lows*, 279–89. A Deepak, Hampton, VA.

Shuchman, R. A., E. G. Josberger, C. A. Russel, K. W. Fischer, O. M. Johannessen, J. Johannessen and P. Gloersen, 1998: Greenland Sea Odden sea ice feature: Intra-annual and interannual variability. *Journal Of Geophysical Research-Oceans*, **103**, 12709–12724.

Skeie, P., 2000: Meridional flow variability over the Nordic seas in the Arctic Oscillation framework. *Geophysical Research Letters*, **27**, 2569–2572.

Skeie, P. and S. Grønås, 2000: Strongly stratified easterly flows across Spitsbergen. *Tellus*, **52A**, 473–486.

Sorteberg, A., N. G. Kvamstø and Ø. Byrkjedal, 2005: Wintertime Nordic Seas Cyclone Variability and Its Impact on Oceanic Volume Transports Into the Nordic Seas. In *The Nordic Seas: An Integrated Perspective*, 137–156. American Geophysical Union.

Thompson, W. and S. Burk, 1991: An investigation of an Arctic front with a vertically nested mesoscale model. *Monthly Weather Review*, **119**, 233–261–.

Wernli, H. and C. Schwierz, 2006: Surface cyclones in the ERA-40 dataset (1958-2001). Part I: Novel identification method and global climatology. *Journal Of The Atmospheric Sciences*, **63**, 2486–2507.

Wilkinson, J. P., 2006: Ice dynamics in the central Greenland sea. *Journal Of Geophysical Research-Oceans*, **111**, C12022.

Wu, B., J. Wang and J. Walsh, 2004: Possible feedback of winter sea ice in the Greenland and Barents Seas on the local atmosphere. *Monthly Weather Review*, **132**, 1868–1876.

Wu, B., J. Wang and J. Walsh, 2006: Dipole anomaly in the winter Arctic atmosphere and its association with sea ice motion. *Journal Of Climate*, **19**, 210–225.

Zhang, X. D., J. E. Walsh, J. Zhang, U. S. Bhatt and M. Ikeda, 2004: Climatology and interannual variability of arctic cyclone activity: 1948-2002. *Journal Of Climate*, **17**, 2300–2317.